



HAL
open science

Offretite zeolite single crystals crystallized using amphiphile-templating approach

Eng-Poh Ng, Nur Hidayahni Ahmad, Fitri Khoerunnisa, Svetlana Mintova,
Tau Chuan Ling, T. Jean Jean Daou

► **To cite this version:**

Eng-Poh Ng, Nur Hidayahni Ahmad, Fitri Khoerunnisa, Svetlana Mintova, Tau Chuan Ling, et al..
Offretite zeolite single crystals crystallized using amphiphile-templating approach. *Molecules*, 2021,
26 (8), pp.2238. 10.3390/molecules26082238 . hal-03414931

HAL Id: hal-03414931

<https://hal.science/hal-03414931>

Submitted on 4 Nov 2021

HAL is a multi-disciplinary open access archive for the deposit and dissemination of scientific research documents, whether they are published or not. The documents may come from teaching and research institutions in France or abroad, or from public or private research centers.

L'archive ouverte pluridisciplinaire **HAL**, est destinée au dépôt et à la diffusion de documents scientifiques de niveau recherche, publiés ou non, émanant des établissements d'enseignement et de recherche français ou étrangers, des laboratoires publics ou privés.

Offretite zeolite single crystals crystallized using amphiphile-templating approach

Eng-Poh Ng^{1,*}, Nur Hidayahni Ahmad,¹ Fitri Khoerunnisa,² Svetlana Mintova,³ Tau-Chuan Ling,⁴ T. Jean Daou^{5,6,*}

¹*School of Chemical Sciences, Universiti Sains Malaysia, 11800 USM, Penang, Malaysia.*

²*Department of Chemistry, Universitas Pendidikan Indonesia, Setiabudi 229, Bandung, 40154, West Java, Indonesia.*

³*Laboratoire Catalyse & Spectrochimie, ENSICAEN, Université de Caen, 14000 Caen, France.*

⁴*Institute of Biological Sciences, Faculty of Science, University of Malaya, 50603 Kuala Lumpur, Malaysia.*

⁵*Université de Haute-Alsace, Axe Matériaux à Porosités Contrôlées, Institut de Science de Matériaux de Mulhouse UMR 7361, ENSCMu, 3b rue Alfred Werner, 68093 Mulhouse, France.*

⁶*Université de Strasbourg, 67000 Strasbourg, France.*

* *Corresponding authors. E-mail address: epng@usm.my (EPN); jean.daou@uha.fr (TJD)*

Abstract

Offretite zeolite synthesis in the presence of cetyltrimethylammonium bromide (CTABr) is reported for the first time. The offretite crystals exhibited novel hexagonal prismatic shape with high crystallinity after only 72 h of hydrothermal treatment at 180 °C which is considerably faster than the already known synthesis procedure used for the preparation of offretite. The study showed that CTABr has dual-functions during crystallization of offretite, *viz.* as structure-directing agent and as mesopore-former. The resulting offretite crystals (Si/Al ratio = 4.1) possess more acid sites than the conventional offretite thanks to its high

crystallinity and hierarchical structure. The synthesized zeolite is also more reactive than its conventional counterpart in the acylation of 2-methylfuran for biofuel production under non-microwave instant heating condition, giving 83.5% conversion with 100% selectivity to the desired product 2-acetyl-5-methylfuran. Hence, this amphiphile synthesis approach offers another cost-effective and alternative route for crystallizing zeolite materials that require expensive organic templates.

Keywords: Hierarchical zeolites; Crystal growth; Offretite zeolite; Amphiphile-templating approach; Acylation of 2-methylfuran

1 Introduction

Zeolites are crystalline microporous materials made up of tetrahedral TO_4 (T = Si or Al) repeating units [1]. These porous solids are widely used in catalysis, separation and ion exchange processes due to their unique structure with defined size and shape [2–4]. 253 types of zeolite structures have been recognized by the International Zeolite Association (IZA) so far [5]. The synthesis of zeolites can be achieved by using various techniques such as organotemplating [6, 7], organotemplate-free [8, 9], ionothermal [10, 11], interconversion [12, 13], ADOR (Assembly, Disassembly, Organization and Reassembly) [14, 15] and fluoride routes [16, 17].

Offretite zeolite (OFF topology) is a 12-membered ring zeolite (diameter $6.7 \times 6.8 \text{ \AA}^2$) with 3-dimensional channel system. It is considered as a very important zeolite due to its very large pore channels that allows ease molecular diffusion and accessibility [18]. To our Knowledge, offretite can only crystallize in the presence of tetramethylammonium (TMA^+) as structure-directing agent (SDA) and both NaOH and KOH as mineralizers [19]. However,

this zeolite seldom crystallizes completely free from erionite (ERI) and analcime (ANA) intergrowth, making the synthesis of pure OFF phase a challenge [20].

Recently, a new strategy for synthesizing offretite has been reported using new SDAs (pyrocatechol [21], p-dioxane [22]). The resulting crystals possess different morphologies (oval, hexagonal, broccoli-like, prismatic) with merely microporosity thanks to the unique properties (e.g. size, shape, polarity, etc.) of the SDAs. Furthermore, offretite can also be readily crystallized *via* interzeolite conversion method using benzyltrimethylammonium hydroxide as organic template but the method is tedious and produces small amount of erionite as competing phase [23]. Thus, any initiative to crystallize offretite zeolite with high purity using facile synthesis approach is highly appreciated.

In the present work, we applied a combined rational strategy to synthesize large offretite single crystals with hierarchical porosity using a cationic amphiphile template (cetyltrimethylammonium bromide, CTABr) where the hydrophilic head of the amphiphile serves as a SDA for the growth of the zeolite while its hydrophobic tail generates mesoporosity allowing the formation of hierarchical zeolite (micro/mesoporosity). It should therefore have superior adsorption and catalytic properties than the conventional offretite.

2 Experimental

2.1 Synthesis of CTA^+ -offretite zeolite

A clear aluminate solution was first prepared by dissolving KOH (3.018 g, 85%, Merck), $Al_2(SO_4)_3 \cdot 16H_2O$ (1.442 g, 97%, Acros) and CTABr (1.221 g, 97%, Acros) in distilled water (18.208 g). A clear silicate solution was then prepared by mixing HS-40 (6.875 g, 40% SiO_2 , Sigma-Aldrich) with distilled water (9.958 g). The hydrogel with a final molar ratio of $20SiO_2:1Al_2O_3:10K_2O:1.46CTABr:800H_2O$ formed after mixing the silicate and aluminate solutions was aged under stirring (18 h, 25 °C, 500 rpm) and crystallized (180

°C, 72 h). The solid product was filtered, purified (by washing with distilled water) until a pH of 7 and calcined (550 °C, 6 h). Then, the obtained solid (3.000 g) was further ion-exchanged with NH₄NO₃ solution (1 M) and calcined (500 °C, 4 h) to produce protonated offretite zeolite. For comparison, classical TMA⁺-offretite zeolite was also synthesized using tetramethylammonium salt (TMACl) as a SDA [24] and the protonated form zeolite was prepared using the same protocol.

2.2 Characterization

The XRD patterns were recorded with a PANalytical X'Pert PRO diffractometer (Cu K α radiation, $\lambda = 0.15418$ nm, 40 kV, 10 mA, step size = 0.02°, scan speed = 0.2 °/min, scanning range $2\theta = 3^\circ$ – 30°). The morphological properties of zeolite samples were studied using a JEOL JSM-6701F FESEM microscope operating at 20 kV. The chemical composition (Si/Al ratio) of zeolite was estimated using IR spectroscopy technique [25]. The porous properties of solids were studied using a Micromeritics ASAP 2010 instrument. Prior to measurement, the powder sample (ca. 0.07 g) was degassed at 300 °C for 12 h before N₂ adsorption was carried out at –196 °C. The total surface area was computed using the Brunauer–Emmett–Teller (BET) equation whereas the external surface area and micropore volume were calculated using the t-plot model. The total pore volume of the samples was determined by using the amount of N₂ uptake at the relative pressure (p/p°) of 0.996. The acidity of samples was investigated with a BELCAT-B temperature programmed desorption (TPD) instrument. First, the powder sample (ca. 0.07 g) was outgassed at 400 °C overnight before the cell was saturated with NH₃ gas at 25 °C for 30 min. The non-adsorbed NH₃ was then evacuated before the sample was heated and desorb slowly from 25 °C to 600 °C with a heating rate 10 °C/min.

2.3 *Catalytic study*

Offretite zeolite (0.300 g, 400 °C, 4 h), 2-methylfuran (4.7 mmol, Merck) and acetic anhydride (14.1 mmol, Merck) were first added into a 10-mL glass vial. The vial was inserted into a non-microwave instant heating reactor (Monowave 50) and instantly heated to 170 °C for 40 min; less than 2 min was required to reach up the desired temperature. After cooling, the reaction solution was isolated using microfiltration and analyzed with an Agilent's GCMS-5975 Turbo System and 7890A GC-FID.

3 **Results and discussion**

Initially, the crystallization was carried out at 180 °C for 40 h. The XRD results revealed that the solid product remained amorphous after 40 h of heating, indicating that the crystallization of offretite zeolite is an activated process which requires induction stage. At 72 h, the amorphous solid completely transformed into offretite zeolite and no other crystalline phase, such as erionite or merlinoite, was co-crystallized (Fig. 1b). When the XRD pattern of offretite zeolite synthesized using CTA^+ (CTA^+ -offretite) is compared with those of simulated and conventional synthesized ones, the XRD peaks intensity of CTA^+ -offretite are different due to the preferred crystal growth orientations (Fig. 1a,c) [26]. The crystallization process was also performed in the absence of CTABr. However, pure LTL-type zeolite was obtained showing the significant role of CTABr in directing the formation of offretite zeolite.

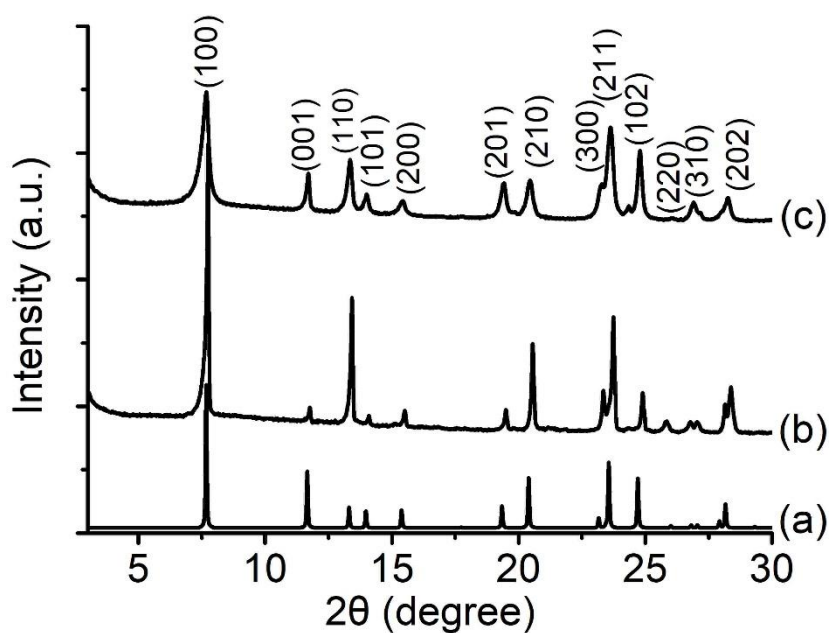


Fig. 1 XRD patterns of (a) theoretical offretite, (b) CTA⁺-offretite and (c) TMA⁺-offretite zeolites.

The SEM images of offretite zeolites prepared using amphiphile templating route are shown in Fig. 2a,b. As seen, this method successfully produces offretite single crystals of hexagonal prismatic shape (inset of Fig. 2a). The surface of CTA⁺-offretite crystals at *a*- and *b*-directions are smooth indicating that the crystals are grown along the *c*-direction [27], forming crystals of $10.8 \times 1.4 \mu\text{m}^2$ length size with an aspect ratio of 7.7. Interestingly, the morphology of the zeolite crystals is different from that of classical TMA⁺-offretite zeolite which exhibits rice grain-shape (ca. $4.6 \times 3.4 \mu\text{m}^2$) which composes of intergrown acicular primary nanocrystals (ca. $880 \times 79 \text{nm}^2$) (Fig. 2c,d). The smaller crystallite size of TMA⁺-offretite zeolite agrees with the XRD peak broadening effect [28] (Fig. 1c).

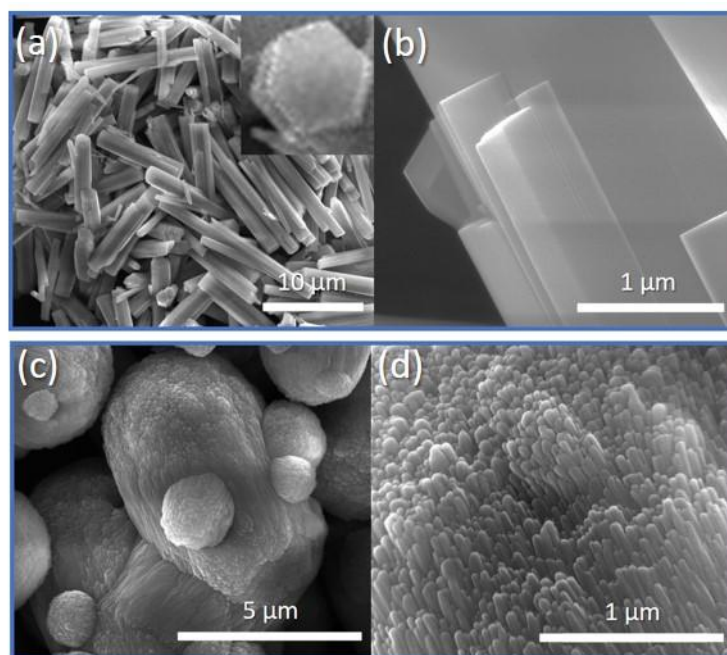


Fig. 2 SEM images of (a, b) CTA⁺-offretite and (c,d) TMA⁺-offretite zeolites under different magnifications.

Offretite zeolite is very useful in the catalytic reactions due to its large pore size and considerably high Si/Al ratio (> 3). According to the IR spectroscopy analysis, the Si/Al ratio of CTA⁺-offretite zeolite is 4.1. Its molecular formula is calculated to be $K_{3.4}Al_{3.4}Si_{14}O_{36}$ which is very close to those of TMA⁺-offretite synthesized in the presence of KOH and NaOH mineralizers ($Na_{1.7}K_{1.7}H_{0.6}Al_4Si_{14}O_{36}$, Si/Al = 3.5) and theoretical one ($Na_{0.2}K_{0.9}Al_4Si_{14}O_{36}$, Si/Al = 3.50) (Table 1) [5]. The textural properties of CTA⁺ and TMA⁺ synthesized offretite zeolites were studied using nitrogen adsorption-desorption analysis. The calcined CTA⁺-offretite solid exhibits a combination of type I and IV adsorption isotherms indicating the presence of micro- and mesoporosities in the solid [29] (Fig. 3a). As a result, multimodal pore size distribution is shown thanks to the role of CTABr as a mesoporegen besides acting as structure-directing agent for the formation of offretite zeolite (inset of Fig. 3a). The zeolite also has higher specific surface area ($S_{BET} = 523 \text{ m}^2/\text{g}$), micropore surface

area ($S_{\text{Mic}} = 503 \text{ m}^2/\text{g}$) and total pore volume ($V_{\text{tot}} = 0.26 \text{ cm}^3/\text{g}$) as compared to the conventional TMA^+ -offretite zeolite ($S_{\text{BET}} = 504 \text{ m}^2/\text{g}$, $S_{\text{Mic}} = 491 \text{ m}^2/\text{g}$, $V_{\text{Tot}} = 0.19 \text{ cm}^3/\text{g}$), which strongly supports the high crystallinity of CTA^+ -offretite zeolite (Fig. 3b).

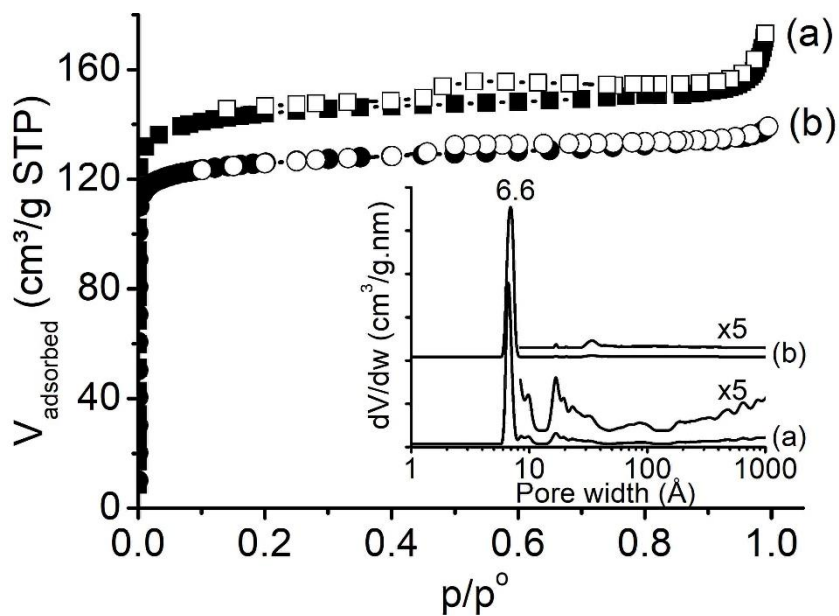


Fig. 3 Nitrogen adsorption-desorption isotherms and (inset) pore size distributions of (a) CTA^+ -offretite and (b) TMA^+ -offretite zeolites.

Table 1 Properties of offretite zeolites.

Samples	Si/Al	S_{BET} (m ² /g)	S_{Mic} (m ² /g)	S_{Ext} (m ² /g)	V_{Tot} (cm ³ /g)	NH ₃ -TPD acidity (mmol/g)			
						T _{des,150 °C}	T _{des,200 °C}	T _{des,350 °C}	Total
CTA ⁺ -offretite	4.1	523	503	20	0.26	0.18	0.24	0.32	0.74
TMA ⁺ -offretite	3.5	504	491	13	0.19	0.17	0.26	0.25	0.68

It is suggested that CTA^+ has dual functions during crystallization process. First, the trimethylamine group ($\text{R-N}(\text{CH}_3)_3^+$, $4.26 \times 2.99 \text{ \AA}^2$ [30]) of CTA^+ , which has nearly similar molecular size/dimensions as TMA^+ ($\text{N}(\text{CH}_3)_4^+$, $4.25 \times 3.70 \text{ \AA}^2$ [30]), directs the formation of OFF framework structure *via* restricted electrostatic interaction with the silicoaluminate anionic oligomers (Fig. 4). The inorganic intermediate species then enfold the CTA^+ hydrophilic head, thus inducing nucleation points for long-range propagation and crystallization of offretite zeolite. Secondly, the CTA^+ cation also serves as a porogen by forming irregular micelles, whereby the hydrophobic tails point to each other leading to the formation of mesopores of wide distribution [31].

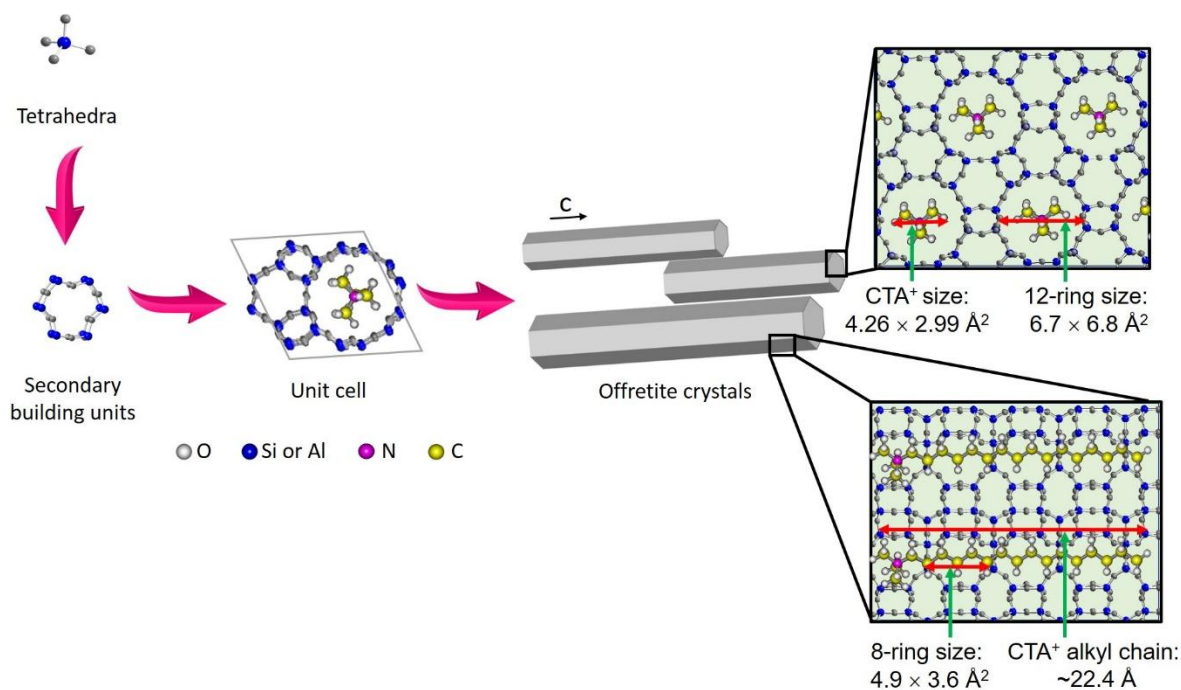


Fig. 4 Formation mechanism of offretite zeolite templated by CTA^+ cation. K^+ cations are not shown for simplicity.

The calcined CTA^+ -offretite has surface acidity after converting into protonated form (Fig. 5). Hence, NH_3 -TPD analysis was used to study the acidity of the zeolite samples. As shown, both the CTA^+ - and TMA^+ -offretites have almost similar amount of weak ($T_{\text{des},150 \text{ }^\circ\text{C}} =$

0.18 mmol/g) and mild ($T_{\text{des},200\text{ }^\circ\text{C}} = 0.25\text{ mmol/g}$) acid sites. Nevertheless, the CTA^+ -offretite contains much larger amount of strong acid sites ($T_{\text{des},350\text{ }^\circ\text{C}} = 0.32\text{ mmol/g}$) than the TMA^+ -offretite (0.68 mmol/g) which could be due to its higher crystallinity and larger accessible (due to the hierarchical structure) surface area [32].

CTA^+ -offretite is suitable to be used as a solid acid catalyst. Hence, its acid properties are tested in the acylation of 2-methylfuran under novel non-microwave instant heating condition (170 °C, 40 min) where the desired product 2-acetyl-5-methylfuran is a useful biofuel additive. The conversion is very low (12%) when no catalyst is added indicating that acylation of 2-methylfuran is an activated reaction and hence requires a catalyst to overcome the activation energy [33] (Table 2, Entry 1). When hierarchical CTA^+ -offretite is added, the conversion increases tremendously to 83.5% with 100% selectivity towards 2-acetyl-5-methylfuran (molecular size $6.6 \times 4.1\text{ \AA}^2$ [30]) (Entry 2). The catalytic performance of CTA^+ -offretite is also compared with that of classical TMA^+ -offretite using the same reaction conditions. As expected, when using CTA^+ -offretite, the reaction conversion (83.5%) is higher than that of TMA^+ -counterpart (78.3%) thanks to its larger surface acidity and the higher accessibility of the acid sites (Entry 4). Thus, the data shows the importance of hierarchical porosity for enhanced bulk molecule diffusivity and accessibility.

The catalytic activity of CTA^+ -offretite is also compared with those of conventional homogeneous catalysts (e.g. HCl, HNO_3 , CH_3COOH). The results show that CTA^+ -offretite has comparable catalytic activity to HNO_3 (83.6% conversion) and it exhibits even better catalytic activity than HCl (72.3%) and CH_3COOH (47.1%) after 40 min of reaction (Entries 5–7). Most importantly, the CTA^+ -offretite zeolite shows high catalyst reusability after the catalytic reaction where no significant loss in catalytic reactivity is observed even after 5 consecutive runs (Entry 3). Thus, the strategy of synthesizing offretite zeolite with

hierarchical structure by amphiphile-templating synthesis route is successful offering safer, cheaper, facile and scale-up feasibility comparing to the previous works [34].

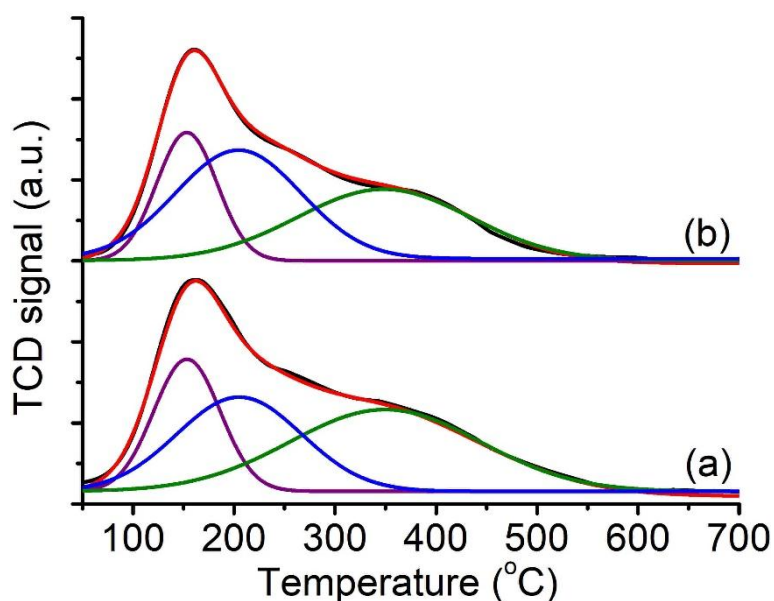


Fig. 5 NH₃-TPD profiles of (a) CTA⁺-offretite and (b) TMA⁺-offretite zeolites.

Table 2 Catalytic performance of catalysts in acylation of 2-methylfuran at 170 °C under non-microwave instant heating conditions.

Entry	Catalysts	Conversion (%)		
		10 min	20 min	40 min
1	No catalyst	3.2	6.4	12.0
2	CTA ⁺ -offretite	52.6	72.3	83.5
3	CTA ⁺ -offretite ^a	50.2	68.0	79.1
4	TMA ⁺ -offretite	44.7	61.7	78.3
5	HCl	35.7	55.3	72.3
6	HNO ₃	51.1	71.9	83.6
7	CH ₃ COOH	16.0	31.9	47.1

^aAfter 5th run.

4 Conclusion

In conclusion, offretite zeolite with high crystallinity has been successfully synthesized *via* amphiphile-templating approach. By using cetyltrimethylammonium bromide (CTABr) as a promising structure-directing agent (SDA), where its hydrophilic head has nearly the same dimensions as tetramethylammonium (TMA^+), offretite zeolite crystals with hexagonal prism shape ($10.8 \times 1.4 \mu\text{m}^2$) are crystallized at 180°C after 72 h of hydrothermal treatment. The resulting zeolite has larger surface areas, pore volume and pore sizes thanks to CTABr that also serves as a mesoporegen. Furthermore, CTA^+ -offretite (0.74 mmol/g) has higher acidity than the conventional TMA^+ -offretite (0.68 mmol/g) and its acidity and accessible porosity are highly appreciated in the acylation of 2-methylfuran with 83.5% conversion and 100% selectivity to the desired product after 40 min reaction at 170°C under non-microwave instant heating conditions. Most importantly, the CTA^+ -offretite catalyst is reusable and more active than conventional TMA^+ -offretite and homogeneous acid catalysts. Hence, the current study is beneficial for zeolite community as this amphiphile-templating strategy using other amphiphilic compounds can be applied in the preparation of many important zeolites that are normally synthesized using harmful and expensive organic templates.

Acknowledgement

The financial support from RUI (1001/PKIMIA/8011128) and Institut Universitaire de France (IUF) is acknowledged.

References

- [1] M. Dusselier, M.E. Davis *Chem. Rev.* **118**, 5265-5329 (2018)

- [2] S.-F. Wong, K. Deekomwong, J. Wittayakun, T.C. Ling, O. Muraza, F. Adam, E.-P. Ng, *Mater. Chem. Phys.* **196**, 295-301 (2017)
- [3] J. Liu, W. Luo, H. Cao, L. Weng, G. Feng, X.-Z. Fu, J.-L. Luo, *Micropor. Mesopor. Mater.* **306**, 110409 (2020)
- [4] K.-H. Tan, H. Awala, R.R. Mukti, K.-L. Wong, T.C. Ling, S. Mintova, E.-P. Ng, *J. Taiwan Inst. Chem. Eng.* **58**, 565-571 (2016)
- [5] International Zeolite Association Web site, <http://www.iza-online.org/>
- [6] E. Catizzone, M. Migliori, T. Mineva, S. van Daele, V. Valtchev, G. Girodano, *Micropor. Mesopor. Mater.* **296**, 109987 (2020)
- [7] L. Tosheva, E.-P. Ng, S. Mintova, M. Hözl, T.H. Metzger, A.M. Doyle, *Chem. Mater.* **20**, 5721-5726 (2008)
- [8] Y. Wang, Q. Wu, X. Meng, F.-S. Xiao, *Engineering* **3**, 567-574 (2017)
- [9] E.-P. Ng, H. Awala, J.-P. Ghoy, A. Vicente, T.C. Ling, Y.H. Ng, S. Mintova, F. Adam, *Mater. Chem. Phys.* **159**, 38-45 (2015)
- [10] E.R. Cooper, C.D. Andrews, P.S. Wheatley, P.B. Webb, P. Wormald, R.E. Morris, *Nature* **430**, 1012-1016 (2004).
- [11] E.-P. Ng, L. Itani, S.S. Sekhon, S. Mintova, *Chem: Eur. J.* **16**, 12890-12897 (2010).
- [12] M. Itakura, K. Ota, S. Shibata, T. Inoue, Y. Ide, M. Sadakane, T. Sano, *J. Cryst. Growth* **314**, 274-278 (2011)
- [13] C.-R. Boruntea, L.F. Lundegaard, A. Corma, P.N.R. Vennestrom, *Micropor. Mesopor. Mater.* **278**, 105-114 (2019)
- [14] M. Trachta, P. Nachtigall, O. Bludsky, *Catal. Today* **243**, 32-38 (2015)

- [15] J. Prech, J. Cejka, *Catal. Today* **277**, 2-8 (2016)
- [16] P. Caullet, J.-L. Paillaud, A.S. Masseron, M. Soulard, J. Patarin, *CR Chim.* **8**, 245-266 (2005)
- [17] A. Matijasic, V. Gramlich, J. Patarin, *Solid State Sci.* **3**, 155-167 (2001)
- [18] J.A. Gard, J.M. Tait, *Acta Cryst.* **B28**, 825-834 (1972)
- [19] K.A. Lukaszuk, D.R. -Gama, S.O. -Odegaard, A. Lazzarini, G. Berlier, S. Bordiga, K.P. Lillerud, U. Olsbye, P. Beato, L.F. Lundegaard, S. Svelle, *Catal. Sci. Technol.* **7**, 5435-5447 (2017)
- [20] Sanyuan Yang, N.P. Evmiridis, *Micropor. Mater.* **6**, 19-26 (1996)
- [21] F. Gao, X. Li, G. Zhu, S. Qui, B. Wei, C. Shao, O. Terasaki, *Mater. Lett.* **48**, 1-7 (2001)
- [22] A. Matijasic, J. Patarin, *Micropor. Mesopor. Mater.* **29**, 405-412 (1999)
- [23] M. Itakura, Y. Oumi, M. Sadakane, T. Sano, *Mater. Res. Bull.* **45**, 646-650 (2010)
- [24] S. Mintova, "Verified Syntheses of Zeolitic Materials", 3rd Ed., Amsterdam: Elsevier Science, 2016.
- [25] Y.-K. Ma, S. Rigolet, L. Michelin, J.L. Paillaud, S. Mintova, F. Khoerunnisa, T.J. Daou, E.-P. Ng, *Micropor. Mesopor. Mater.* **311**, 110683 (2021)
- [26] X. Wang, P. Karakilic, X. Liu, M. Shan, A. Nijmeijer, L. Winnubst, J. Gascon, F. Kapteign, *ACS Appl. Mater. Interfaces* **10**, 33574-33580 (2018)
- [27] K.A. Łukaszuk, D. Rojo-Gama, S. Øien-Ødegaard, A. Lazzarini, G. Berlier, S. Bordiga, K.P. Lillerud, U. Olsbye, P. Beato, L.F. Lundegaard, S. Svelle, *Catal. Sci. Technol.* **7**, 5435-5447 (2017)
- [28] S.-F. Wong, H. Awala, A. Vincente, R. Retoux, T.C. Ling, S. Mintova, R.R. Mukti, E.-P. Ng, *Micropor. Mesopor. Mater.* **249**, 105-110 (2017)
- [29] E.-P. Ng, L. Delmotte, S. Mintova, *Green Chem.* **10**, 1043-1048 (2008)

- [30] The molecular size of the compounds were estimated using HyperChem™-Release 8.0 for Windows Molecular Modeling System, Hypercube, Inc., 2011.
- [31] D. Ali, C.R. Zeiger, M.M. Azim, H.L. Lein, K. Mathisen, *Micropor. Mesopor. Mater.* **306**, 110364 (2020)
- [32] J. Přeč, K.N. Bozhilov, J.E. Fallah, N. Barrier, V Valtchev, *Micropor. Mesopor. Mater.* **280**, 297-305 (2019)
- [33] T.M.A. Ghrear, S. Rigolet, T.J. Daou, S. Mintova, T.C. Ling, S.H. Tan, E.P. Ng, *Micropor. Mesopor. Mater.* **227**, 78-83 (2019)
- [34] D.P. Serrano, J.M. Escola, P. Pizarro, *Chem. Soc. Rev.* **42**, 4004-4035 (2013)